Reconstructing fracture progression in impact

Mike W. J Arun, S. Mukherjee and A. Chawla

Department of Mechanical Engineering, Indian Institute of Technology Delhi, New Delhi 110016, India

Abstract - Bone fracture patterns could be crucial in reconstructing the nature of loading, especially in the lower limb and upper limb kinematics in vehicle-pedestrian crashes. In addition, use of FE bone models can be a handy tool to predict vehicle impact velocity and the impact direction. The point of fracture initiation in bone loading has been predicted quite accurately earlier. A methodology that predicts bone crack initiation and its propagation pattern for the six known loading directions using a single material and failure model is presented.

INTRODUCTION

Types of fractures in bone differs with impact direction and impact velocity [1, 2]. This property of bone can be exploited for reconstructing the nature of loading and impact speed. The different classifications of fractures are listed in Figure 1. The three point bending test is widely used to characterize bending behavior of materials [3, 4]. In vehicle-pedestrian crashes bone injuries are also caused due to bending. Three-point bending finite element simulations of long bones under impact have been reported [5, 6], but the direction of impact and types of fractures have not been correlated. To the knowledge of authors no previously published literature is available on prediction of types of fractures based on loading directions using finite element method. However large numbers of literature are available on bone micro mechanics [7-16] which played an important role in the investigation of current work.

Application of principles of dynamic fracture mechanics (DFM) give good results when specimens are modeled in 2D [17]. It is not as convenient to use DFM for 3D specimens and when the crack is loaded in mixed modes. Additionally, fracture mechanics analysis is done using an initial crack. As predicting crack initiation is one of the objectives; an initial crack cannot be defined a priori. This limits the applicability of the DFM approach.

The objective of this work is to predict the types of bone fractures for different loading directions (Anterior-A, Posterior-P, Lateral-L, Medial-M) using a single material and failure model, and thereby using the methodology as a reconstructing tool in vehicle-pedestrian crashes.

METHOD

Mesh

The mesh of a finite element model of human femur has been developed using CT scan data [18-22]. The CT scans were obtained using a GE high speed scanner (80 kV, 120 mA, 0.6 mm slice thickness, 512 x 512 matrix). A surface mesh is obtained from the CT scan data using Mimics^{TM}. The surface mesh was converted to solid mesh using Hypermesh^{TM} after cleaning up duplicate and intersecting triangles from the surface mesh. The solid mesh consists of 54,575 linear tetrahedral elements, 14,847 nodes with approximately 3 elements through the radius. The supports and impactor are modeled with rigid elements. The model is assigned a varying density and Young's modulus based on the Hounsfield number from CT scan as proposed by [23]. The length of the femur from the medial condyle to the head of the femur is 410 mm. The highest outer diameter in the mid-diaphysis region is 23 mm and the highest inner diameter is 8 mm.

Experiment description

Suitability of two failure criteria, (1) equivalent plastic strain (using 2% strain as critical strain) (2) dilatational cut-off stress (using 50 MPa critical stress), has been evaluated. Kress et al., have reported six different impact conditions from two different setups [1] . The first setup contains a pneumatic accelerator which propels a cart (50 kg) toward the specimen at a velocity of 7.5 m/s. An instrumented pipe of diameter 4.13 cm and length 10 cm is fixed to the cart front (Figure 2a). In the second setup the pipe is swung like a pendulum (Figure 2b). In both setups and in all cases of impact the specimen is impacted in the mid-shaft region and the specimen is simply supported. Fracture patterns in six cases including, A-P, P-A, L-M, M-L impacts using setup-1 and A-P, L-M impacts using setup-2 were reported. In our work we have simulated these cases and reconstructed the type of fracture reported by them.

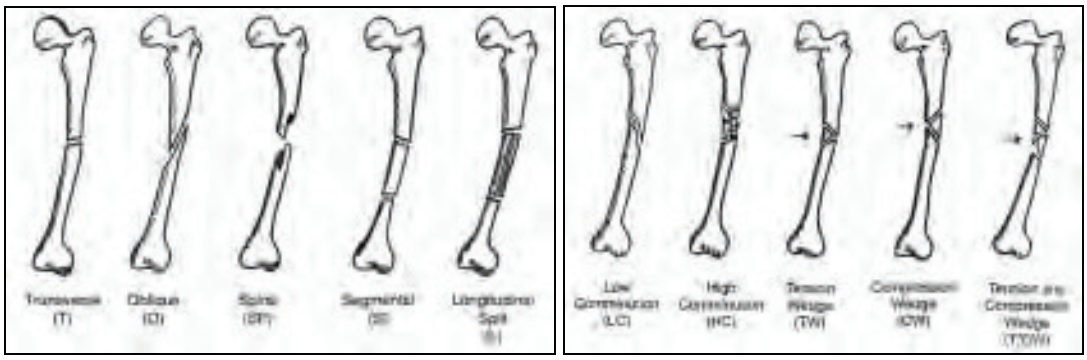

Figure 1 Different types of fractures (both figures adapted from [1])

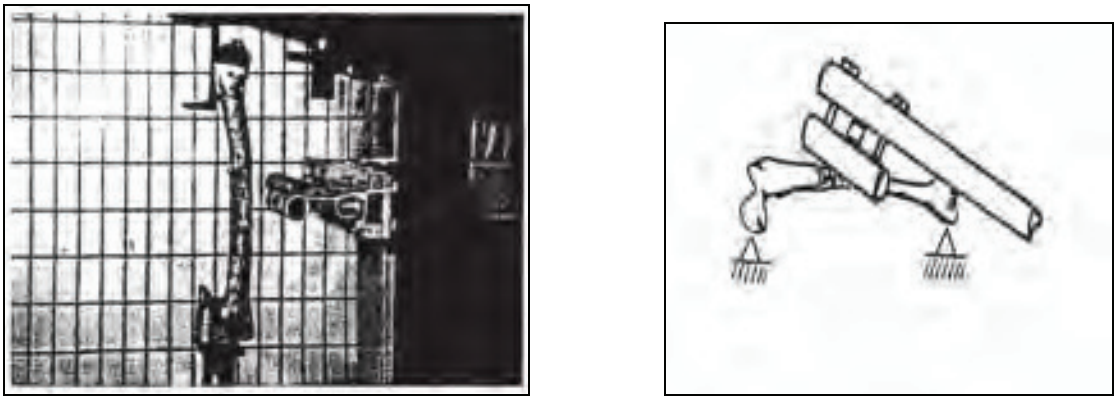

Figure 2 (a) The cart setup (b) The pendulum setup. (both figures adapted from [1])

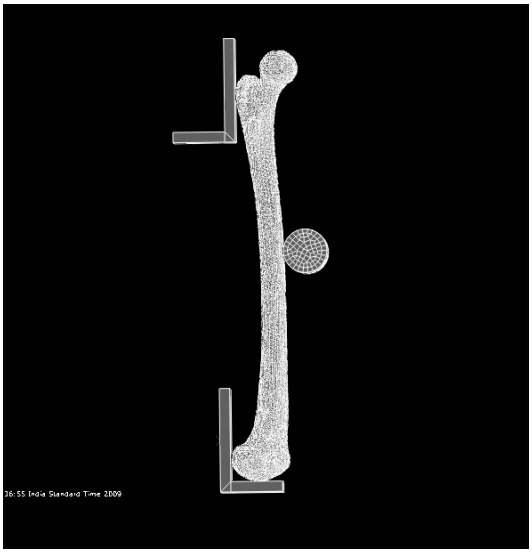

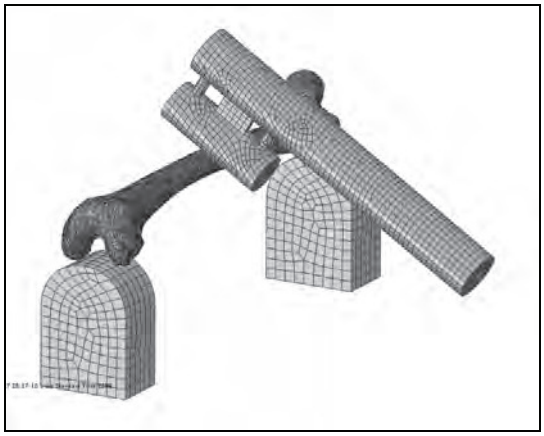

Figure 3 (a) The cart setup (b) The pendulum setup

Finite element model

The corresponding finite element model setup is shown in Figure 3. The most commonly used fracture criterion for long bones is equivalent plastic strain criteria. When the model was simulated using equivalent plastic strain criterion, irrespective of loading directions and the experimental setup the bone *always* fractured transversely and often propagated from the point of impact. Then the model was simulated using dilatational cut-off stress as fracture criteria. This criterion uses the dilatational stress as a failure measure to model dynamic failure. The failure criterion assumes that failure occurs when the dilatational stress, becomes more tensile than the user-specified dilatational cutoff stress[24]. As bones are weaker in tension compared to compression [25-29], it can be expected that the tensile behavior of bone contributes more to its failure. It is also suggested that dilatational stress plays a major role in yielding and failure of porous materials like bone [30]. The average bending strength of femur is 147 Mpa[31] . The dilatational cut-off stress is taken as the one third of the bending strength [32] , which is 50 MPa, for the reconstruction..

RESULTS

Using the proposed dilatational cut off stress criterion, all six cases were simulated. In all the cases the crack initiated from the tensile side as in the experimental cases. Four of the six cases were P-A, L-M, M-L loadings were reproduced well (Figure 4). For P-A plane of impact the FE model resulted in tensile wedge fracture (Figure 4a) where the fracture initiated from the tensile side at two places and propagated towards the compressive side at an angle with the vertical with opposite slopes resembling wings of a butterfly. Hence it is also called as butterfly fracture which is shown in Figure 1 as TW. For L-M and M-L plane of impact the FE model resulted in oblique fracture which is seen in the field. Oblique fractures initiate from the tensile side frequently at an offset from the line of impact (Figure 4b-d) and propagates towards the compressive side at an angle to the vertical which is shown in Figure 1 as O.

It is reasonable to assert that the fractures were predicted well because it is generally accepted that if the maximum angle between the propagated crack and the plane of cross – section is greater than

30˚ [33] then the fracture is oblique type. The angle of oblique, tensile wedge fractures produced during reconstruction was confirmed to be above 30˚. The two A-P loading cases were not reconstructed by the model. Segmental and transverse fracture which is reported to be a lower probability event [1] is also reproduced by the current model (Figure 5). The limiting stress had to be decreased to 45 MPa to reproduce oblique and increased to 55 MPa to reproduce comminuted fractures as seen in the field (Figure 6). This is a 10% variation over the nominal value and is in line with the tensile strength variation reported (80 Mpa to 240 Mpa) [6] for human bones.

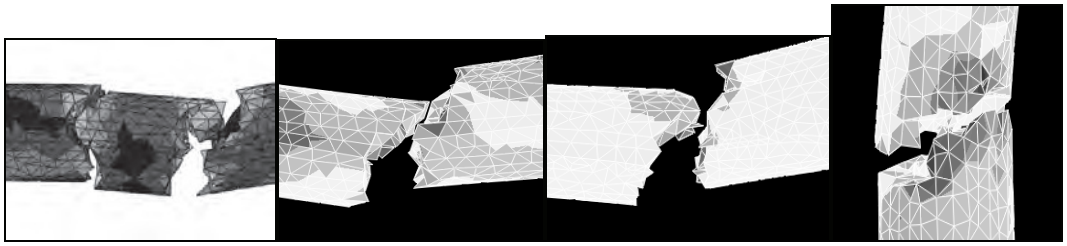

(a) (b) (c) (d)

Figure 4 Simulation results for different impact directions with a cut-off stress of 50 Mpa (a) Tensile wedge, P-A, Pendulum setup (b) Oblique, L-M, Pendulum setup (c) Oblique, M-L, Pendulum setup (d) Oblique, L-M, Cart setup.

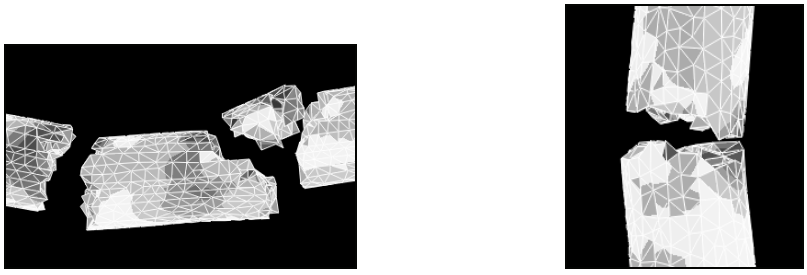

(a) (b)

Figure 5 Simulation results for A-P impact direction for 50 Mpa cut-off stress (a) Segmentation, Pendulum setup (b) Transverse, Cart setup

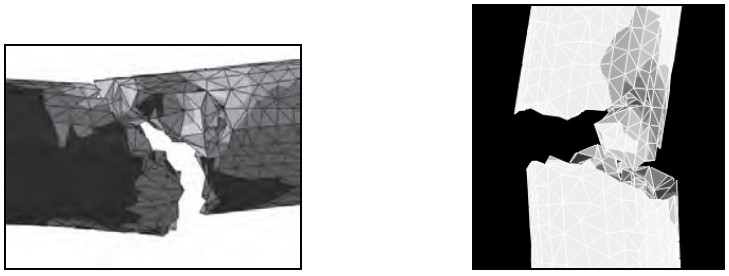

(a) (b)

Figure 6 Simulation results for A-P impact direction for different cut-off stress (a) Oblique, 55 Mpa, Pendulum setup (b) Comminution, 45 Mpa, Cart setup

DISCUSSION

Out of the six cases for which simulation was done, fracture was reconstructed for four of the cases. In the two cases where the impact was in the A-P direction, the model predicted segmental and transverse fractures when 50MPa critical stress was used. However, on varying the critical stress between 45 and 55MPa (± 10% of 50MPa) variation in the type of fracture was observed. At 55MPa and 45MPa oblique and comminution fractures were predicted for pendulum and cart setup respectively, which matched with the experimental results.

This critical stress may vary due to bone porosity, density and elastic modulus variation from subject to subject. There is thus a need to conduct fresh experiments so that specimen specific models can be made for correlating simulation results.

Table 1 shows experimental results of the peak contact force for dynamic three point bending tests conducted on male femur with an average age of 69.2, 83.5, 69.3, 76.3 for A-P, P-A, L-M, M-L plane of impact respectively [1]. Figure 7 shows the comparison of peak contact force between experiment and simulation. It can be observed from the figure that in all cases the current FE model over estimated the peak impact force, however the predicted values lie within the range of standard deviation reported which makes reasonable to assume that this variation may be due to the difference between the material properties of bones reported in experiments and in the reconstruction.

Impact plane	Peak contact force (kN)	SD (kN)	n
A-P	5.70	2.68	50
P-A	2.48	0.69	14
L-M	4.75	4.07	10
M-L	2.29	1.25	9

Table 1 Experimental results of dynamic 3- point bending for male femur using pendulum setup[1]

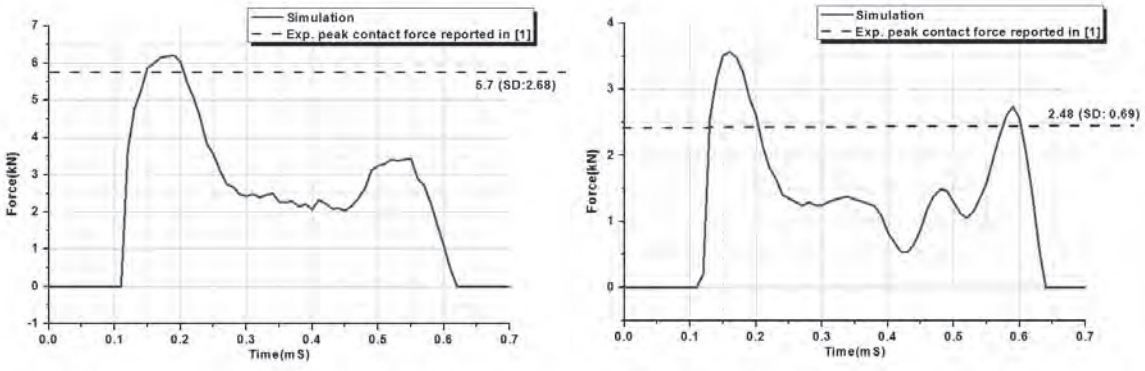

(a) (b)

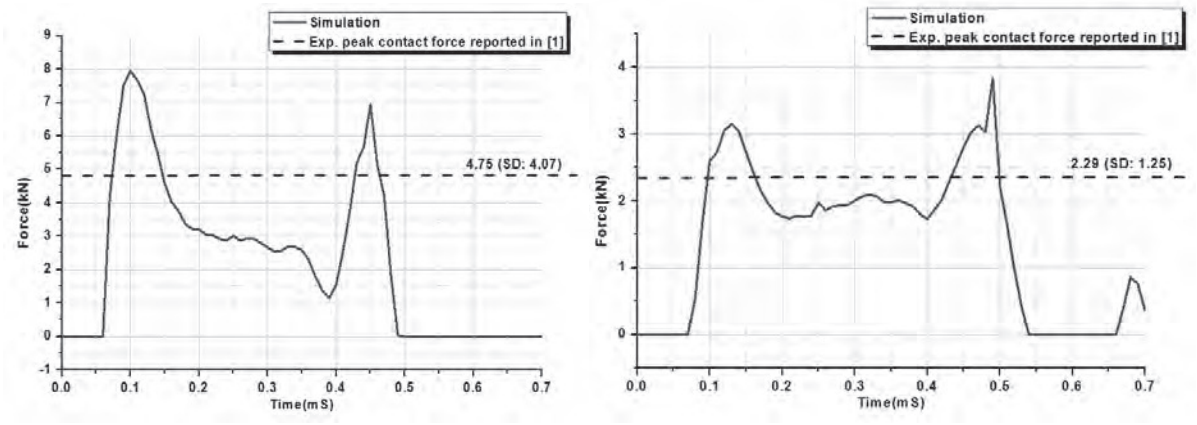

(c) (d)

Figure 7 Comparison of peak contact force in impact direction between experiment [1] and simulation for male femur in different impact plane using pendulum setup(a) A-P (b) P-A (c) L-M (d) M-L

To study the variation fracture types with angular orientation, more simulations were carried out by impacting the bone model at fixed angular interval of 22.5° over a full circle with the same impact speed as earlier. The results are shown in Figure 8, the arrow line indicates the direction and point of impact. It is of interest to note that impact at 157.5° and 202.5° angle of impact (having the anterior plane as reference) produced tensile-compression wedge fracture which is the most infrequently reported fracture type. This fracture is similar to tensile wedge but there is a second crack initiation point and the crack propagates towards the compression side giving rise to a chunk which is an inverted tensile wedge (Figure 1 T/C W).

It is not clear why two types of setups were used as reported in [1]. However for impact with the same geometry of the impactor and the same impact speed the two setup at times produced different types of fracture. For example in the A-P plane of impact, the cart setup produced comminution fracture and pendulum setup produced oblique fracture in both experiment and simulation. The peak contact forces for the pendulum set up was 6.2 kN and cart setup it was 5.9 kN in the simulation. The contact area was not the same for both the cases. Figure 9 shows the contact area between the impactor and the specimen for the two cases. For the cart setup, the contact area is 22mm^2 which is smaller than the pendulum setup (Figure 9a). The cart impactor contacts the apex (Figure 8) of the anterior side of the long bone leading to stress concentration and stress localization. This is perhaps why the result was a comminution fracture which originates from local failure. In the pendulum setup, as the hammer approaches from the side, the impactor hits the relatively flatter surface of the bone in the A-L side (Figure 8) which results in a contact area of 80 mm^2 (Figure 9b) which is about four times the contact area in the cart setup and eventually drops to 20 mm^2 (Figure 9b), however the maximum contact area of 80 mm^2 is attained during the time of the peak contact force This phenomenon reduces stress concentration in the vicinity of contact and avoided comminution fracture, instead producing oblique fracture.

From contact force history obtained from the simulations (Figure 7) it is seen that in all the planes of impact two peaks were observed. The first peak is observed when the impactor first contacts the specimen. The specimen starts to accelerate. Therefore, momentarily, there is a drop in contact force and the impactor makes its second contact with the specimen and the second peak is observed. In all the planes of impact after the second contact the bone fails and the contact force drops to zero. It is interesting to observe that the bone did not fail after the first peak. For A-P, P-A and L-M planes of impact, the magnitude of the second peak is lesser than the first peak. But for M-L plane of impact the magnitude of the second peak is higher.

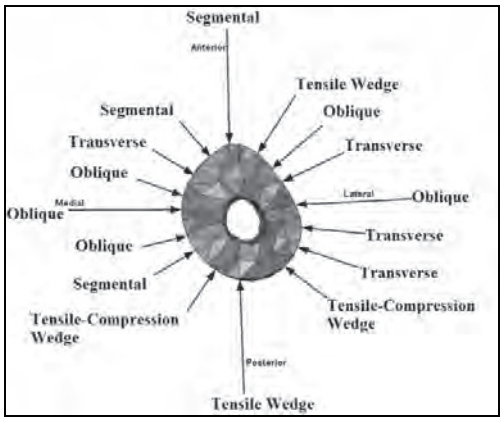

Figure 8 Cross-section of mid-shaft bone region showing the change in types of fracture when bone is impacted at an interval of 22.5˚

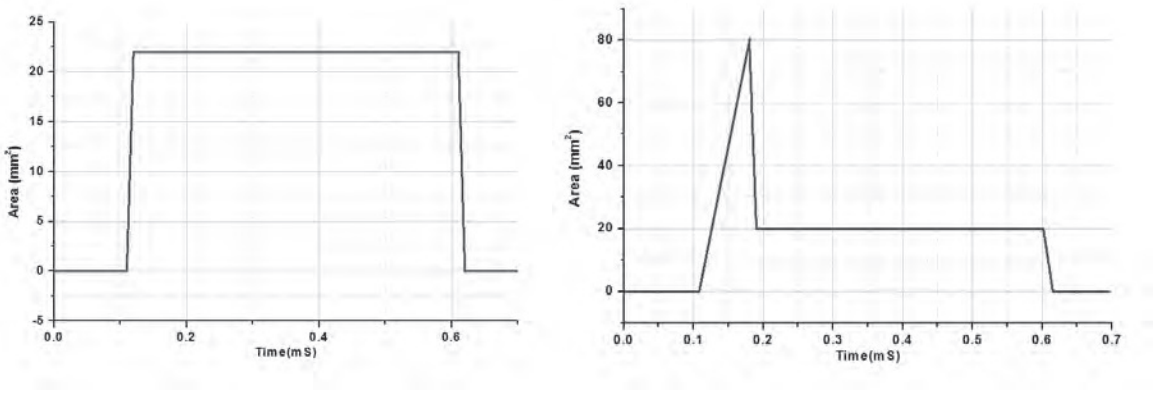

(a) (b)

Figure 9 Contact area between the impactor and specimen in A-P plane of impact for (a) cart setup (b) pendulum setup

LIMITATIONS OF STUDY

A femur model has been used to investigate fracture initiation and pattern due to bending loading. Other loadings like torsion are yet to be investigated. This study was additionally limited by use of isotropic material properties as the CT data currently used does not allow us to generate anisotropic bone properties. Finally the failure criterion used is also isotropic as information in published literature is insufficient as of now to implement anisotropic failure criterion.

CONCLUSION

As fracture type prediction can be considered as a promising tool in reconstructing fracture progression there is a need for a failure criterion with which fracture types can be predicted using a single material and failure model. Material models like elasto-plastic[34, 35], visco-elasic[34-36] have been used to model long bones. Currently equivalent plastic strain criterion is widely used as a failure criteria for long bones. The main setback of this criterion is that it always results in a transverse fracture. Consequently reconstruction of bone fractures for different loading directions using a single material and failure model has not been reported earlier. Additional failure criteria for static cases are also available in literature, viz, strain based criteria[37, 38] and stress based criteria [39] . A failure criterion based on the

tensile part of dilatational stress is shown to be a good predictor of the fracture pattern. The following conclusions can be drawn based on the current work:

1. Six cases which were reported in [1] were reconstructed with the proposed failure criteria. Among the six, four cases were reproduced well and the other two A-P impact cases were also reproduced by tweaking the parameters of the failure criteria.
2. Oblique, Tensile wedge, Tensile-Compression wedge, transverse fractures are initiated by tensile failure. The different progression patterns can then be attributed to influences like plane of bending, direction of loading, impact speed, loading non-linearity etc. Comminution fracture may be caused by high speed impacts or higher stress concentration and/or stress localization.
3. In simulation, two peaks were observed in the contact force history wherein the first peak is higher than the second peak in A-P, P-A and L-M planes of impact while for the M-L plane of impact the second peak is higher than the first.
4. Bones always failed after the second peak in the contact force history.
5. The functional difference between the two experimental setups reported in [1] was investigated and it is found to be that the area of contact between the impactor and the specimen is different for the two setups. This is perhaps one of the main reasons why the impact in the A-P plane in two setups resulted in different fracture types.
6. To study the variation fracture types with angular orientation, more simulations were carried out by impacting the bone model at fixed angular interval of 22.5° over a full circle with an impact speed of 7.5 m/s. The transition/Boundary where one fracture type changes to another is identified.
7. Critical dilatational cut-off stress failure criteria would be a better predictor of crack progression as compared to strain based failure criteria.

ACKNOWLEDGEMENTS

The authors acknowledge the support from the Transportation Research and Injury Prevention Program (TRIPP) at Indian Institute of Technology Delhi for providing part of the infrastructure used in the work.

REFERENCES

1. Kress TA, Porta DJ, Snider JN, Fuller PM, Jennie PP, Heck WL, Frick SJ, Wasserman JF. Fracture patterns of long bones in human cadaver. In: Proceedings of International Research Council on Biomechanics of Injury conference. 155. 1995
2. Koval KJ, Zuckerman JD. Handbook of Fractures: Lippincott Williams & Wilkins, 2006
3. Jiang F, Vecchio KS. Experimental investigation of dynamic effects in a two-bar/three-point bend fracture test. Review of Scientific Instruments 78(6): 063903, 2007
4. Cordey J. An introduction to selected chapters in bone biomechanics. Injury 30(Supplement 1): SA1, 1999
5. Untaroiu CD. Development and validation of a finite element model of human lower limb. In.: University of Virginia. 2005
6. Takahashi Y, Kikuchi Y, Konosu A, Ishikawa H. Development and Validation of the Finite Element Model for the Human Lower Limb of Pedestrians. In: 44th Stapp Car Crash Conference. 2000
7. Dubey DK, Tomar V. Microstructure dependent dynamic fracture analyses of trabecular bone based on nascent bone atomistic simulations. Mechanics Research Communications 35(1-2): 24,
8. Martin RB, Lau ST, Mathews PV, Gibson VA, Stover SM. Collagen fiber organization is related to mechanical properties and remodeling in equine bone. A comparsion of two methods. Journal of Biomechanics 29(12): 1515, 1996
9. Martin RB, Boardman DL. The effects of collagen fiber orientation, porosity, density, and mineralization on bovine cortical bone bending properties. Journal of Biomechanics 26(9): 1047, 1993
10. Martin AVW. Electron microscope studies of collagenous fibres in bone. Biochimica et Biophysica Acta 10: 42, 1953
11. Turner CH, Chandran A, Pidaparti RMV. The anisotropy of osteonal bone and its ultrastructural implications. Bone 17(1): 85, 1995
12. Rodrigues CVM, Serricella P, Linhares ABR, Guerdes RM, Borojevic R, Rossi MA, Duarte MEL, Farina M. Characterization of a bovine collagen-hydroxyapatite composite scaffold for bone tissue engineering. Biomaterials 24(27): 4987, 2003

13. Cusack S, Miller A. Determination of the elastic constants of collagen by Brillouin light scattering. Journal of Molecular Biology 135(1): 39, 1979
14. Saino H, Luther F, Carter DH, Natali AJ, Turner DL, Shahtaheri SM, Aaron JE. Evidence for an extensive collagen type III proximal domain in the rat femur : II. Expansion with exercise. Bone 32(6): 660, 2003
15. Luther F, Saino H, Carter DH, Aaron JE. Evidence for an extensive collagen type III/VI proximal domain in the rat femur: I. diminution with ovariectomy. Bone 32(6): 652, 2003
16. Wang X, Bank RA, TeKoppele JM, Mauli Agrawal C. The role of collagen in determining bone mechanical properties. Journal of Orthopaedic Research 19(6): 1021, 2001
17. Voyiadjis GZ, Kattan PI. Damage Mechanics: Taylor & Francis Group, 2005
18. Guy P, Krettek C, Mannss J, Whittall KP, Schandelmaier P, Tscherne H. CT-based analysis of the geometry of the distal femur. Injury 29(Supplement 3): 16, 1998
19. Aamodt A, Kvistad KA, Andersen E, Lund-Larsen J, Eine J, Benum P, Husby OS. Determination of the Hounsfield value for CT-based design of custom femoral stems. J Bone Joint Surg Br 81-B(1): 143, 1999
20. Wardlaw JM, Best JJK, Hughes SPF. Dynamic bone imaging in the investigation of local bone pathology -- When is it useful? Clinical Radiology 43(2): 107, 1991
21. Brown S, Bailey DL, Willowson K, Baldock C. Investigation of the relationship between linear attenuation coefficients and CT Hounsfield units using radionuclides for SPECT. Applied Radiation and Isotopes 66(9): 1206, 2008
22. Biondetti PR, Vannier MW, Gilula LA, Knapp RH. Three-dimensional surface reconstruction of the carpal bones from CT scans: Transaxial versus coronal technique. Computerized Medical Imaging and Graphics 12(1): 67,
23. Rho JY, Hobatho MC, Ashman RB. Relations of mechanical properties to density and CT numbers in human bone. Medical Engineering & Physics 17(5): 347, 1995
24. Simulia. Abaqus Manual 6.9. In.:
25. Sirois I, Cheung AM, Ward WE. Biomechanical bone strength and bone mass in young male and female rats fed a fish oil diet. Prostaglandins, Leukotrienes and Essential Fatty Acids 68(6): 415, 2003
26. Shim VPW, Yang LM, Liu JF, Lee VS. Characterisation of the dynamic compressive mechanical properties of cancellous bone from the human cervical spine. International Journal of Impact Engineering 32(1-4): 525, 2005
27. Burgers TA, Mason J, Niebur G, Ploeg HL. Compressive properties of trabecular bone in the distal femur. Journal of Biomechanics 41(5): 1077, 2008
28. George WT, Vashishth D. Damage mechanisms and failure modes of cortical bone under components of physiological loading. Journal of Orthopaedic Research 23(5): 1047, 2005
29. Mahnken R. Strength difference in compression and tension and pressure dependence of yielding in elasto-plasticity. Computer Methods in Applied Mechanics and Engineering 190(39): 5057, 2001
30. Hu LW, Pae KD. Inclusion of the hydrostatic stress component in formulation of the yield condition. Journal of the Franklin Institute 275(6): 491, 1963
31. Kress TA, Snider JN, Porta DJ, Fuller PM, Wasserman JF, G.V.Tucker. Human femur response to impact loading In: IRCOBI. 1993
32. Leclère G, Nême A, Cognard JY, Berger F. Rupture simulation of 3D elastoplastic structures under dynamic loading. Computers & Structures 82(23-26): 2049,
33. Bucholz RW, Heckman JD, Court-Brown C. Rockwood and Green's Fractures in Adults Lippincott Williams & Wilkins
34. Natali AN, Carniel EL, Pavan PG. Constitutive modelling of inelastic behaviour of cortical bone. Medical Engineering & Physics 30(7): 905, 2008
35. Phillips A, Pankaj P, May F, Taylor K, Howie C, Usmani A. Constitutive models for impacted morsellised cortico-cancellous bone. Biomaterials 27(9): 2162, 2006
36. Zhang J, Niebur GL, Ovaert TC. Mechanical property determination of bone through nano- and micro-indentation testing and finite element simulation. Journal of Biomechanics 41(2): 267, 2008
37. Nalla RK, Stölken JS, Kinney JH, Ritchie RO. Fracture in human cortical bone: local fracture criteria and toughening mechanisms. Journal of Biomechanics 38(7): 1517, 2005
38. Majumder SR, Mazumdar S. Mechanical breakdown of trabecular bone: Dependence on microstructure. Physica A: Statistical Mechanics and its Applications 377(2): 559, 2007
39. Keyak JH, Rossi SA. Prediction of femoral fracture load using finite element models: an examination of stress- and strain-based failure theories. Journal of Biomechanics 33(2): 209, 2000